Science of the Total Environment 590-591 (2017) 370–380

Contents lists available at ScienceDirect

Science of the Total Environment

journal homepage: www.elsevier.com/locate/scitotenv

Data-driven mapping of the potential mountain permafrost distribution

Nicola Deluigi*, Christophe Lambiel, Mikhail Kanevski

Institute of Earth Surface Dynamics, University of Lausanne, Lausanne, Switzerland

HIGHLIGHTS

- Investigation of an innovative permafrost distribution modelling approach
- Three classifiers belonging to statistics and machine learning were applied.
- Machine learning algorithms provide precise distribution maps at the micro-scale.
- Predicted permafrost distribution is in accordance with the field reality.

GRAPHICAL ABSTRACT

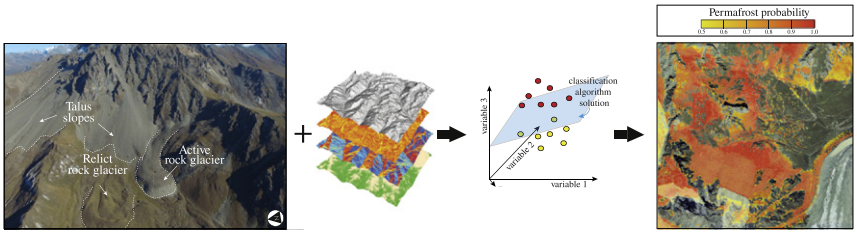

Dataset: positive/negative permafrost evidences and related permafrost predictors

Machine learning classifier (learning from data)

Permafrost prediction

ARTICLE INFO

Article history:
Received 31 October 2016
Received in revised form 3 February 2017
Accepted 5 February 2017
Available online 8 March 2017

Keywords:
Mountain permafrost
Classification algorithms
Machine learning
Mapping

ABSTRACT

Existing mountain permafrost distribution models generally offer a good overview of the potential extent of this phenomenon at a regional scale. They are however not always able to reproduce the high spatial discontinuity of permafrost at the micro-scale (scale of a specific landform; ten to several hundreds of meters). To overcome this lack, we tested an alternative modelling approach using three classification algorithms belonging to statistics and machine learning: Logistic regression, Support Vector Machines and Random forests. These supervised learning techniques infer a classification function from labelled training data (pixels of permafrost absence and presence) with the aim of predicting the permafrost occurrence where it is unknown. The research was carried out in a 588 km^2 area of the Western Swiss Alps. Permafrost evidences were mapped from ortho-image interpretation (rock glacier inventorying) and field data (mainly geoelectrical and thermal data). The relationship between selected permafrost evidences and permafrost controlling factors was computed with the mentioned techniques. Classification performances, assessed with AUROC, range between 0.81 for Logistic regression, 0.85 with Support Vector Machines and 0.88 with Random forests. The adopted machine learning algorithms have demonstrated to be efficient for permafrost distribution modelling thanks to consistent results compared to the field reality. The high resolution of the input dataset (10 m) allows elaborating maps at the micro-scale with a modelled permafrost spatial distribution less optimistic than classic spatial models. Moreover, the probability output of adopted algorithms offers a more precise overview of the potential distribution of mountain permafrost than proposing simple indexes of the permafrost favorability. These encouraging results also open the way to new possibilities of permafrost data analysis and mapping.

1. Introduction

Within the 21st century, the Alpine environment is going to experience deep modifications of the cryosphere as a consequence of the increase in air temperatures and the modifications of precipitation regimes. Among the cryospheric components, mountain permafrost describes a ground with temperatures at or below 0°C for two consecutive years (Harris et al., 2009; Beniston et al., 2017). Permafrost in rock walls and sedimentary accumulations may degrade as a consequence of the climate change (Etzelmüller and Frauenfelder, 2009). A thickening of the active layer and a warming of the permafrost body can have various effects on mountain

* Corresponding author.
E-mail address: nicola.deluigi@unil.ch (N. Deluigi).

http://dx.doi.org/10.1016/j.scitotenv.2017.02.041
0048-9697/

slope stabilities, such as an increasing rock fall activity (Gruber and Haeberli, 2007; Ravanel et al., 2010) or a rock glacier acceleration (Kääb et al., 2007; Roer et al., 2008; Delaloye et al., 2010; PERMOS, 2016), leading to an increase of the sediment transfer rates (Lane et al., 2007; Kobierska et al., 2011).

In the European Alps, the periglacial belt is generally marked by the absence of trees, a reduced vegetation cover (where existing essentially made of meadow, mosses and lichens), large volumes of sediment debris, steep slopes and rock faces. Although permafrost may affect all these different types of terrains, its unambiguous morphological manifestation only occurs in active rock glaciers, which are considered as the visible expression of mountain permafrost creep (Haeberli, 1985). Other permafrost indicators are thrust- or push-moraines, corresponding to frozen sediments deformed by the glacier advance during the Little Ice Age, whereas large areas in glacier forefields located in the periglacial belt appear to be unfrozen (Reynard et al., 2003; Harris and Murton, 2005; Kneisel and Kääb, 2007; Bosson et al., 2015). Talus slopes constitute other major landforms of alpine environments where permafrost is generally restricted to the lower half of the slope (e.g. Lambiel and Pieracci, 2008; Otto and Sass, 2006; Scapozza et al., 2011). It is also well established that terrains covered by alpine meadow are generally permafrost free (Haeberli, 1975). The distribution of mountain permafrost is thus extremely discontinuous in mountain areas (see also Ribolini et al., 2010; Otto et al., 2012).

The ability of modelling the spatial distribution of such a complex phenomenon became an important task for the alpine permafrost research during the last two decades. First empirico-statistical models were based on simple approaches (such as linear regression) and offered a good overview of the potential distribution of mountain permafrost at the regional scale (i.e. Hoelzle, 1994; Ebohon and Schrott, 2008; Avian and Kellerer-Pirklbauer, 2012). These models are generally thresholding the occurrence of permafrost on the basis of a restricted number of topographical and climatic parameters (i.e. altitude of rock glacier fronts for a given orientation) and are validated with measurements of the ground surface temperature, which may be subject to bias. The availability of an increasing amount of high resolution data (generally derived from high resolution digital elevation models) opened then the way to new complex statistical models able to deal with a large number of predictors (i.e. Boeckli et al., 2012; Schöner et al., 2012; Magnin et al., 2015; Azócar et al., 2016; Sattler et al., 2016). Although they offer a good overview of the permafrost distribution at local scale (i.e. scale of a valley side), these models do not reflect the great heterogeneity of the phenomenon at the scale of a specific landform (the micro-scale; covering ten to several hundreds of meters).

To address the need of an improved prediction of the permafrost extent at the micro-scale, we propose an alternative approach, which employs classification algorithms belonging to statistics and machine learning, namely Logistic regression, Support Vector Machines and Random forests. These algorithms can deal with complex and high dimensional datasets (Bishop, 2006) and they derive functional dependencies directly from data without appealing to physical models (Hastie et al., 2009). They have successfully been adopted for mapping the spatial distribution of several natural phenomena (i.e. Amatulli et al., 2013; Varley et al., 2016). In the periglacial research such techniques have been already used for geomorphological mapping (Luoto and Hjort, 2005), landform characterization (Marmion et al., 2008) or permafrost mapping using satellite images (Ou et al., 2016). Accordingly, we collected field observations indicating the known presence or the known absence of mountain permafrost and related topo-climatic data for a specific area of the Western Swiss Alps. The dataset built was analyzed and used to investigate the potential of machine learning techniques for mapping the high spatial discontinuity of mountain permafrost. Furthermore, as the potential permafrost distribution in rockwalls had already been successfully modelled in other studies (i.e. Gruber et al., 2004; Noetzli et al., 2007; Magnin et al., 2015), the present work focuses only on sedimentary accumulations.

2. Materials and methods

2.1. Permafrost evidences and explanatory variables

This study was carried out in a sector of the Western Valais Alps (Switzerland) covering a regular grid of 588 km^2, with more than 60% above the theoretical permafrost lower limit of 2500 m.a.s.l., delimiting the lower boundary of the periglacial belt in the area (Lambiel and Reynard, 2001).

We used evidences of known permafrost presence or absence collected since the mid-1990s by the Universities of Lausanne and Fribourg as training data for employed machine learning algorithms (Fig. 1). These evidences have been obtained from two distinct sources:

- *Rock glacier inventories*. Permafrost presence or absence can be derived from rock glacier maps, based on their activity. Indeed, active or inactive rock glaciers suggest the existence of permafrost conditions, whereas relict ones indicate its absence (see Haeberli, 1985; Humlum, 1996; Barsch, 2012). For this study, we employed some existing inventories (Delaloye and Morand, 1998; Morand, 2000; Lambiel and Reynard, 2003), for which rock glaciers were mapped directly in the field. Some additional rock glaciers located within the study area were also added through ortho-image interpretation. All rock glacier limits were then corrected with a comparison with recent orthophotos (Swissimage, from swisstopo) and their activity was verified with the analysis of geomorphic signatures and InSAR signals (Delaloye et al., 2007; Barboux et al., 2014).
- *Geoelectrical and thermal data*. Direct-current (DC) resistivity methods are well established tools for detecting permafrost in sediments (Hauck and Kneisel, 2008). Electrical resistivity tomography (ERT) is especially often utilized to detect ground ice and characterize frozen materials in permafrost environments (e.g. Hauck et al., 2003; Hilbich et al., 2009; Otto et al., 2012). In addition, permafrost can also be inferred from ground surface temperature measurements (Hoelzle et al., 1999; Carturan et al., 2015). Coupling geoelectrical and thermal data can thus improve the reliability of permafrost mapping. Following the procedure employed by Lambiel (2006, p. 95) and Scapozza et al. (2011), we compiled and combined geoelectrical and thermal data collected in the framework of different studies aiming at detecting and mapping ground ice in permafrost environments – mainly talus slopes and glacier forefields – of our study area (Marescot et al., 2003; Reynard et al., 2003; Delaloye, 2004; Delaloye and Lambiel, 2005, 2008; Lambiel, 2006; Lambiel and Pieracci, 2008; Scapozza et al., 2011; Scapozza, 2013; Staub et al., 2015). Completed by thermal measurements gathered for the Swiss Permafrost Monitoring Network (PERMOS, 2016) and by other unpublished projects, these data were used to map the permafrost extension in the prospected landforms. This provided to the classification algorithms additional training examples also located outside rock glaciers. Negative training observations (known permafrost absence) resulted not only from in-situ measurements indicating warm conditions or absence of ground ice, but also from expert knowledge. We particularly used the conclusions of Lambiel and Pieracci (2008) and Scapozza et al. (2011) that showed the general absence of permafrost in the upper half of talus slopes.

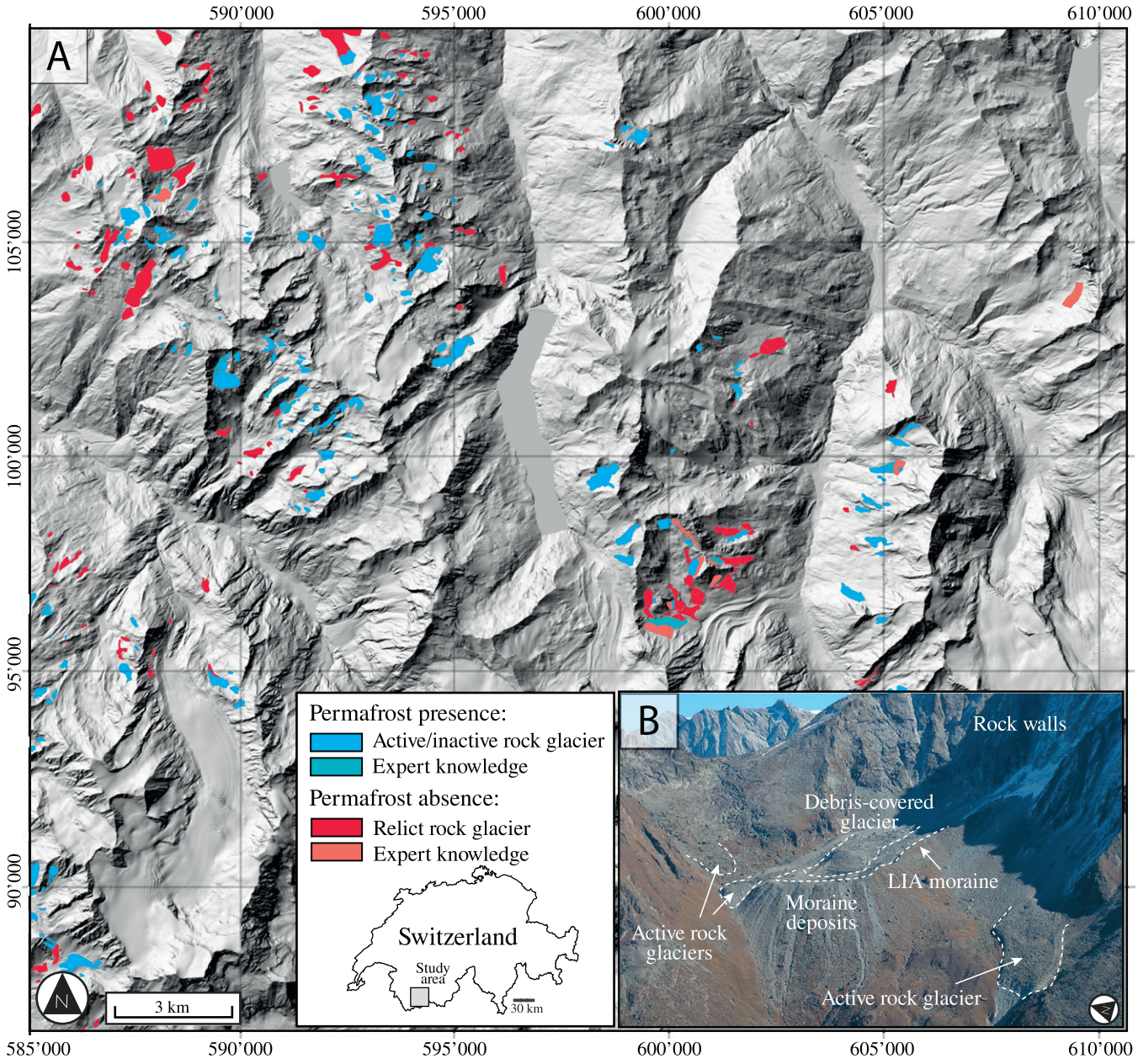

Fig. 1. (A) Extent of the study area (relief map) and localization of known permafrost evidences. (B) Typical Alpine periglacial landscape characterized by active rock glaciers, debris-covered glacier, talus slopes, moraine deposits and rock walls (Arolla Valley, Valais; photo: R. Delaloye).

For this study, we selected environmental variables that are commonly used in the field of permafrost modelling (e.g. Etzelmüller et al., 2001; Guglielmin et al., 2003; Boeckli et al., 2012) such as altitude, mean annual air temperature, aspect, terrain slope angle and potential incoming solar radiation. In addition, we computed the NDVI and the planar, profile and combined terrain curvature indices, which are morphometric predictors important in characterizing specific periglacial landforms such as rock glaciers or moraines. The relevance of selected predictions is presented in the following sub-sections:

- Altitude: Permafrost occurrence increases with the altitude at the regional scale, due to the decrease of the mean annual air temperature (MAAT) at higher altitudes. As MAAT is calculated on the basis on a linear temperature gradient (−0.59°C/100 m above 1500 m, for methodology see Bouët, 1978), these two predictors were extremely correlated (see Fig. 2). Accordingly, to avoid redundancy, the adopted dataset excluded the MAAT variable and only considered the altitude. The latter is derived from the SwissAlti3D digital elevation model from the Swiss Federal Office of Topography (swisstopo). It is a spatial grid with an aperture width of 2 m above 2000 m.a.s.l. and it is produced by stereo correlation with 1–3 m average error. The density of at least 2 points/m^2 avoids noise in the data.
- Aspect: The terrain orientation is also considered extremely relevant for the permafrost presence/absence. Terrains with different aspects have different energy inputs due to a different radiation angle. The amount of energy per unit area can actually vary in a ratio of 1 to 10 between the sunny side and the shady side of a relief. Since terrain orientation is a circular variable (between 0° and 360°), we built two uncorrelated indicators: the "northness", which corresponds to the cosine of aspect angle, and the "eastness", equal to the minus sine of the aspect value (see Brenning and Trombotto, 2006).

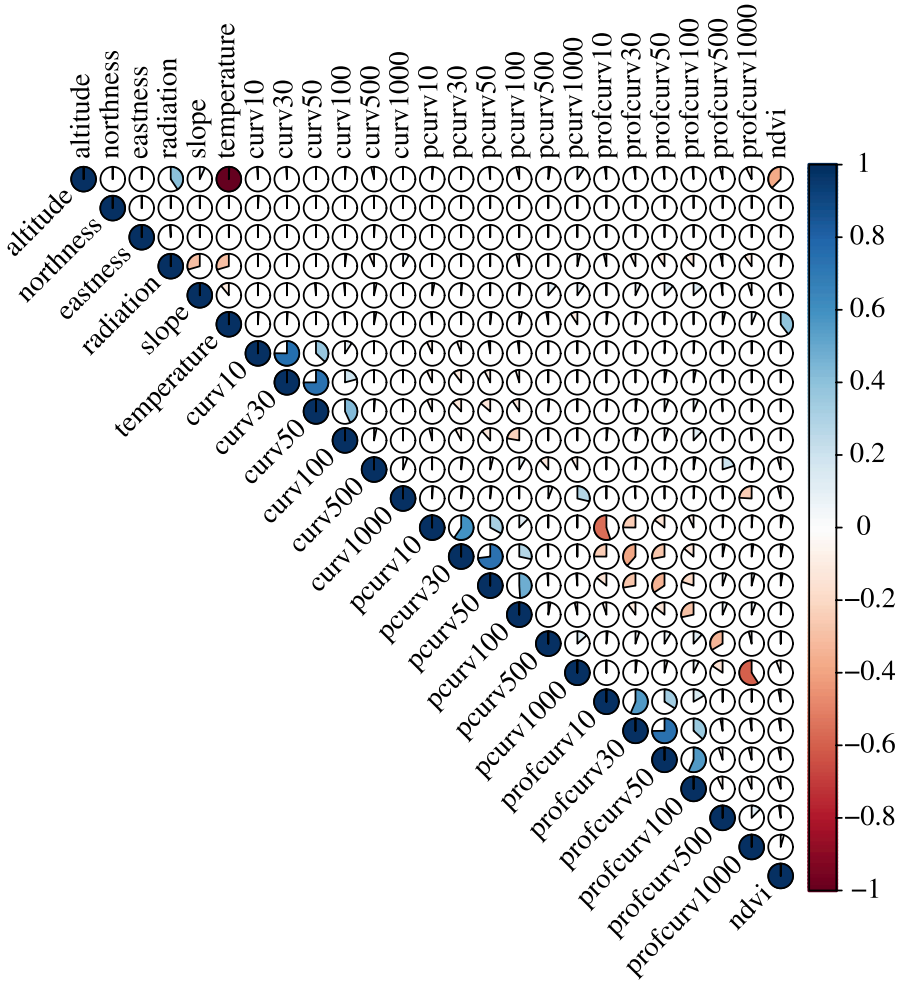

Fig. 2. Correlation plot of selected environmental variables within the validity domain.

- Slope: The terrain slope angle influences the permafrost occurrence by governing the direct solar radiation reaching the ground surface. In addition, snow cover may have different depths depending on the slope: rock walls are generally snow free while flat areas of footslopes may be covered by an important amount of snow (Mittaz et al., 2002).
- Potential incoming solar radiation: The amount of energy reaching the ground was calculated as potential incoming solar radiation (PSIR). For this we used the ArcMap "Area Solar Radiation" tool on the 2 m DEM, taking into account shadowing effect of the relief. PSIR was computed for the snow free period, between the July 1st and October 31st (which usually corresponds to the period without snow cover), because PSIR does not have relevant effects on the ground temperature if the snow is present (Hoelzle, 1994).
- Terrain curvature: As mountain permafrost is a thermal phenomenon, it is only observable with the appearance of geomorphological indices such as rock glaciers lobes or with in-situ measurements. Thus, adding a curvature indicator helps recognizing the presences of lobes that are potentially occupied by permafrost. The Gaussian terrain curvature (the derivative of the slope angle) was computed at different window sizes (10, 30, 50, 100, 500, 1000 m) and was included to the dataset as an indicator of various landforms. Large window curvatures (i.e. concavities) help machine learning algorithms to detect the presence of a valley bottom. Conversely, small window terrain curvatures indicate lobes, crests or small depressions (Fig. 3).
- Normalized Difference Vegetation Index: A Normalized Difference Vegetation Index (NDVI) was also calculated from false-color infrared images (swisstopo) and included in the dataset. This continuous variable is used for differentiating the vegetation from other land types, as well as characterize local variability in sediment textures.

2.2. Adopted dataset

A delimited area in which proposed simulations were run (the so-called validity domain) was defined based on categorical variables. The prediction of the permafrost occurrence was only computed for sectors where the latter is uncertain (the prediction can be either "permafrost absence" or "permafrost presence"), typically in sedimentary accumulations such as talus slopes, moraine deposits or other debris surfaces. Areas were permafrost is generally absent, such as temperate glaciers, rivers, lakes or vegetation areas, were excluded from the validity domain (Table 1).

The dataset was built on a regular grid of 10 × 10 m. Consequently, the original DEM raster and relative extracted predictors controlling the presence and absence of mountain permafrost were resampled by computing the mean value of the 2 × 2 m cells. A spatial resolution of 10 m was selected in reason of the computational requirements needed to predict the permafrost distribution for such an extended study area and the minimum size of typical periglacial landforms, such as rock glacier or moraine ridges, that can be represented with at least 2 pixels (a width of 20 m). A

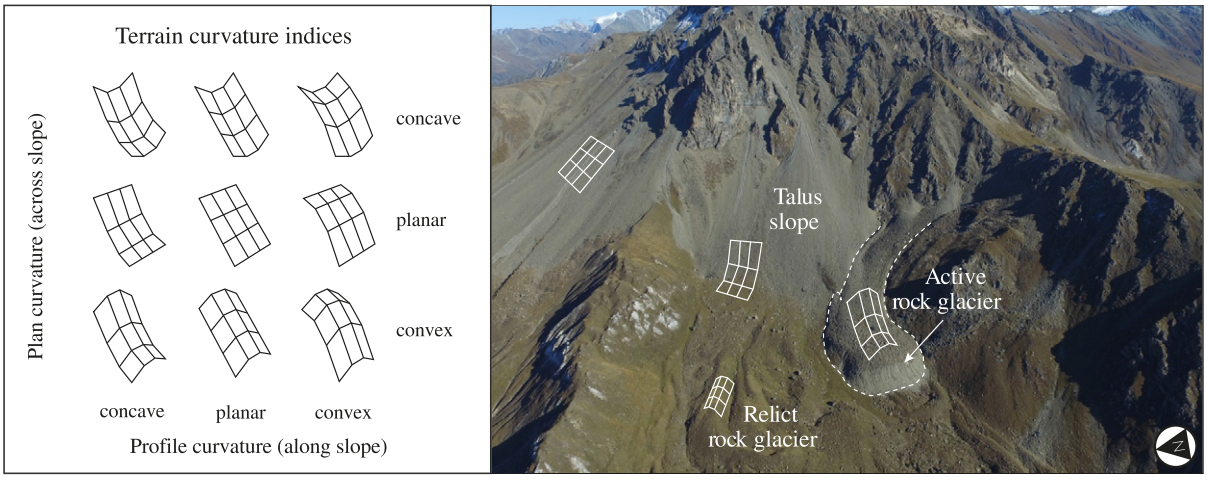

Fig. 3. Terrain curvature types and associated landforms for Les Cliosses sector, with an active rock glacier indicating the presence of permafrost (Hérens Valley, Valais; photo: S. Rüttimann).

higher resolution of the dataset would introduce unexpected noise, both in the attributes (i.e. erroneous attribute values) and the class (label noise, i.e. contradictory examples or miss-classifications). This would require additional preprocessing and noise filtering analysis to reduce the noise's effects. Moreover, due to the complexity of the studied phenomenon, from a physical perspective willing to map the permafrost distribution at a too high resolution is illusory.

2.3. Training, validation and test sets

In the present research, classification algorithms were trained, validated and tested with separate independent sub-sets obtained from the original permafrost dataset. The latter can be considered a benchmark data bank to be used for the analysis of the influence of environmental predictors on the permafrost distribution as well as for the modelling of the potential permafrost distribution with machine learning (both are parts of ongoing research). These sub-sets were selected by sampling individual observations from group of data with different characteristics, previously identified by clustering the original input space (the variable space) with the help of a Self-Organizing Map (SOM, Kohonen, 1982; Kohonen and Honkela, 2007). This type of artificial neural network was trained using unsupervised learning and provided an ordered mapping of the data observations onto a two-dimensional grid. The SOM algorithm computed different models associated with each node of the grid. Observations were mapped into the node whose model is similar to data observation itself. The 2-dimensional map was then clusterized by using the k-means algorithm, while the number of clusters was selected by computing the Davies–Bouldin index (Davies and Bouldin, 1979). By grouping observations with similar characteristics within the input space, a balanced selection from pools of samples with similar characteristics was made. Rather than randomly sampling the permafrost observations, this sampling strategy avoided the presence of highly auto-correlated training samples within the separate sub-sets and produced less classification overfitting.

Table 1
Features contained in the raw dataset. Categorical variables serve constructing the validity domain (VD), continuous variables are used for classifying the permafrost occurrence.

Variable name	Variable type	Use
Altitude	Continuous	Classification
Northness	Continuous	Classification
Eastness	Continuous	Classification
Slope	Continuous	Classification
PSIR	Continuous	Classification
Air temperature	Continuous	Classification
Lake	Categorical	VD definition
Rockwall	Categorical	VD definition
River	Categorical	VD definition
NDVI	Continuous	Class. / VD def.
Plan curvature 10 m	Continuous	Classification
Plan curvature 30 m	Continuous	Classification
Plan curvature 50 m	Continuous	Classification
Plan curvature 100 m	Continuous	Classification
Plan curvature 500 m	Continuous	Classification
Plan curvature 1000 m	Continuous	Classification
Profile curvature 10 m	Continuous	Classification
Profile curvature 30 m	Continuous	Classification
Profile curvature 50 m	Continuous	Classification
Profile curvature 100 m	Continuous	Classification
Profile curvature 500 m	Continuous	Classification
Profile curvature 1000 m	Continuous	Classification
Surface curvature 10 m	Continuous	Classification
Surface curvature 30 m	Continuous	Classification
Surface curvature 50 m	Continuous	Classification
Surface curvature 100 m	Continuous	Classification
Surface curvature 500 m	Continuous	Classification
Surface curvature 1000 m	Continuous	Classification
Glacier	Categorical	VD definition

2.4. Classifiers

In this work, three classifiers were applied to permafrost data. At present, a large palette of classification methods, belonging to statistics and machine learning, exists (Kanevski et al., 2009). For instance, some of these common statistical techniques are the k-nearest neighbor (e.g. Altman, 1992; Everitt et al., 2011), the linear discriminant analysis (e.g. Friedman, 1989) and the logistic regression (see McLachlan, 2004). More recently, other complex algorithms have been developed in order to deal with the emergence of complex set of data and the lack of non-linear solutions. Artificial neural networks, Support Vector Machines and Random forests are just a few examples (Cherkassky and Mulier, 2007; Izenman, 2008; Haykin, 2009; Hastie et al., 2009). These algorithms aim at assigning the class of an observation (here a pixel of the study grid) based on related environmental variables. In order to work, these techniques require a set of training data that are used to fit the classification decision function.

In the following sections, a theoretical overview of Logistic regression (LR), Support Vector Machines (SVM) and Random forests (RF) is given. We selected these algorithms because they belong to three specific sub-domain of machine learning: the former is a linear parametric classifier and it is commonly used as a benchmark classifier to be employed before using more complex classification algorithms. Non-linear SVM is a non-parametric learning algorithm

and it is a member of the so-called kernel methods. Finally, RF are an ensemble learning method based on bootstrap aggregating.

2.4.1. Logistic regression

Logistic regression is one of the most used method for susceptibility mapping in geosciences (see Brenning, 2005; Trigila et al., 2015). This technique fits the best model between independent indicators to dependent variables (Kleinbaum and Klein, 1994). In our case, it tries to estimate the best mathematical relationship between the absence and the presence of permafrost and a set of explanatory independent environmental variables $x_1,\ldots,x_n$, which can be both continuous or categorical (Hosmer and Lemeshow, 2000). The model output for each grid cell represents the probability p to belong to the permafrost presence. It is based on the logistic function p_i, which is defined as follows:

$$logit(p_i) = \log\left[\frac{p_i}{1-p_i}\right] \tag{1}$$

where the likelihood ratio corresponds to the ratio between the probability p that the predicted class is 1 (presence of permafrost) and the probability $1-p$ that the class is 0 (absence of permafrost). The final linear logistic model takes this form:

$$logit(p_i) = \beta_0 + \sum_{i=1}^{n}\beta_i x_i \tag{2}$$

with $\beta_0,\beta_1,\ldots,\beta_n$ the coefficients measuring how each independent environmental variable contributes to the permafrost occurrence.

In the present work, the logistic regression is performed using its implementation in WEKA, which is an improved version of the original algorithm presented in Le Cessie and Van Houwelingen (1994).

2.4.2. Support Vector Machines

Support Vector Machines (SVM) is a machine learning algorithm based on the statistical learning theory developed by Vapnik (1998). It is based on Structural Risk Minimization that minimizes the training error and controls the complexity of the model in order to improve the generalization ability of a model (Cherkassky and Mulier, 2007).

SVM can be applied to classification tasks and non-linear regression problems. The main principle of this technique presupposes that the set of training vectors $D = \{(x_1,y_1),(x_2,y_2),\ldots,(x_n,y_n)\}$ where $x_i \in R^m, i = 1,\ldots,n$ with two classes $y_i = \{-1,1\}$ is linearly separable by a hyper-plane:

$$(w\cdot x) + b = 0, w \in R^N, b \in R \tag{3}$$

where w corresponds to the hyper-plane normal, $(\cdot)$ is a scalar product and b is a scalar base.

The SVM algorithm aims at maximizing the largest margin that separates the training vectors and that is expressed as $\frac{2}{\|w\|}$ after the normalization. The maximum margin is computed as follows:

$$\min_{w,b}\frac{1}{2}\|w\|^2 \tag{4}$$

subjecting to the constrains $y_i(w^T x_i + b) \geq 1, i = 1,2,\ldots,n$. The cost function is expressed as:

$$\phi(w,b;\alpha) = \frac{1}{2}\|w\|^2 - \sum_{i=1}^{n}\alpha_i\,(y_i[w\cdot x_1 + b] - 1) \tag{5}$$

where $\alpha = (\alpha_1,\alpha_2,\ldots,\alpha_n)^T \in R_+^n$ is a Lagrangian multiplier.

As detailed in Vapnik (1998), the problem has to be solved by dual minimization of the cost function with the respect to w and b. Because in most cases the training vectors are rarely linearly separable, a slack variable ξ_i and a penalty term C, avoiding high values of the latter, are introduced:

$$y_i((w\cdot x_i) + b) \geq 1 - \xi_i, i = 1,2,\quad \ldots,n, \xi_i \geq 0 \tag{6}$$

Therefore, the equation, maximizing the margin becomes:

$$\min\frac{1}{2}\|w\|^2 + C\sum_{i=1}^{n}\xi_i. \tag{7}$$

Non-linear classification of real data is performed using the same principles, but only by applying a kernel trick (Vapnik, 1998) when a kernel function $K(x_i,x_j)$ maps/transforms the original data into a high dimensional feature space where, again, we are looking for a linear solution. Depending on the kernel, the linear solution in the feature space corresponds to a non-linear solution in the original space and the kernel controls the complexity of this mapping.

In this work, we used a radial basis function (RBF) kernel $K(x_i,x_j) = e^{\left(-\gamma\left\|x_i-x_j\right\|^2\right)}, \gamma > 0$ which is one of the most used kernels providing a good generalization. Moreover, we employed the libSVM library implemented in WEKA. For additional information on the application of this algorithm, please see Deluigi and Lambiel (2012).

2.4.3. Random forests

Developed by Breiman (2001), Random forests is an ensemble algorithm that computes n binary classification trees (forest) with the purpose of having higher predictive capabilities compared to the classification with a single decision tree (Cutler et al., 2007). With the combination of several trees constructed with a random selection of the inputs, the classification accuracy usually improves. Implemented in WEKA, this technique is suitable when dealing with both categorical and numerical predictors. It adopts bagging to randomly select permafrost observations and their relative variables to train the model. The membership of a class is selected by a majority vote for the most popular class within the total number of trees. In this study, we used by default 2/3 bootstrap of the training set to construct each tree. The remaining 1/3 bootstrap of the training data was used to assess the generalization capacity of the algorithm.

With this technique there is thus no need for a cross-validation or a separate validation set to obtain unbiased estimate of the test set error. Unselected observations serve indeed to calculate the error of the model (the "out-of-bag" error, or OOB). The error estimate also allows measuring the contribution of each predictor by computing the average decrease in model accuracy on the OOB samples when the values of the respective feature are randomly permuted. Two evaluators of the variable importance exist with Random forests: the Mean-Decrease-in-Accuracy, measuring the decrease of the accuracy expressed with the OOB-error when a variable is left out and the Mean-Decrease-in-Gini index, defining how the output at each node is impure (Breiman, 2001).

Because of the random selection of independent variables and observations at each node, analysing the correct number of trees to be employed in Random forests is suggested in order to obtain a stable model (Catani et al., 2013). Therefore, before applying the classification model on a new prediction, we firstly investigated the changes in the OOB error curve, aiming at selecting the correct number of trees (see Section 3.1).

2.5. Classification quality measures

The known permafrost absence and presence was binary coded as $[-1,1]$. Nevertheless, with the chosen classifiers it is possible to obtain the probability of belonging to the class as model output. This result is in fact most convenient when dealing with a natural phenomenon.

The quality of the prediction of the presence and absence of permafrost modelled with supervised learning algorithms can be generally assessed with multiple statistics (Doswell III et al., 1990). As we deal with binary classification, in this study we computed 2-by-2 contingency tables that display four possible cases (see Fig. 4): number of true positives (TP), i.e. a pixel with known permafrost presence that was predicted correctly (presence–presence); true negatives (TN), when absence is correctly not encountered (absence–absence); false negatives (FN), i.e. permafrost presence is not detected (presence–absence) or false positives (FP) for permafrost absence incorrectly forecasted (absence–presence). Indeed, when dealing with the management of natural hazards related to periglacial source areas, it is preferable to obtain a conservative result that misclassifies permafrost where in reality it is not, rather than the opposite.

In addition to these rates, a Receiver Operating Characteristics curve (ROC) can be built (Fawcett, 2006). This 2-dimensional graph measures the quality of the model prediction by plotting the FP rate as the horizontal axis and the TP rate as the vertical axis, according to different susceptibility threshold values. Swets (1988) indicates that the Area Under the ROC curve (or AUROC) ranges between 0.5 and to 1. Values between 0.5 and 0.7 generally indicate that the learned model has poor predictive capabilities.When AUROC is between 0.7 and 0.8, it means that the classification have moderate predictive abilities. Between 0.8 and 0.9 they are considered good and above 0.9 they become excellent. Nevertheless, recent studies have observed that, for similar AUROCs, the predicted map of a given phenomenon can be particularly different (i.e. Micheletti et al., 2014).

2.6. Used softwares

In this research we have used algorithms that are already implemented in WEKA (Waikato University, Hall et al., 2009). The LibSVM library (Chang and Lin, 2011) is implemented in this software as a package. Permafrost evidence identification, variables extraction and dataset building were performed by using ArcGIS (ESRI) and Matlab softwares.

3. Results and discussion

In order to select the best map of the potential distribution of mountain permafrost for the Western part of the Valais Alps, modelling performances of standard Logistic regression were compared to the ones of Support Vector Machines and Random forests. The model setup was characterized by the selection of training and test data including observations of the permafrost presence and permafrost absence coupled together with environmental variable grids. As mentioned, we decided to present the algorithm predictions in the form of probabilities, which provide easiness when comparing different model outputs. Moreover, for coherence with existing models and ease of map comparability, presented maps visualize probabilities greater than 0.5, corresponding to the possible presence of permafrost.

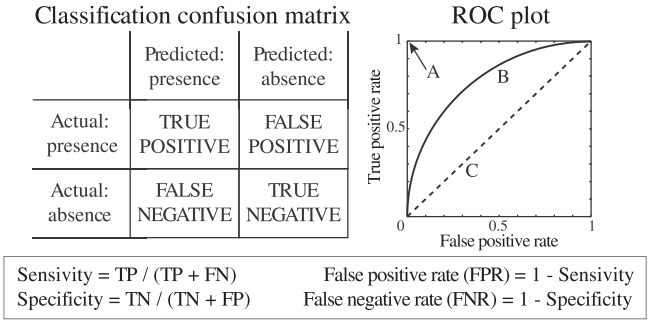

Fig. 4. Classification confusion matrix (left) and evaluation rates (bottom) used to assess the model quality. The Receiver Operating Characteristics curve also indicates the quality of the classification: (A) corresponds to the perfect result (no errors, AUROC = 1), (B) indicates a typical ROC curve (AUROC = 0.85) and (C) refers to an inefficient classification (AUROC = 0.5).

3.1. Model assessment

By removing auto-correlated variables from the dataset (Fig. 2) before applying the Logistic regression, the algorithm converged to a solution, providing an AUROC value of 0.807 (Table 2). The sum of percentage of false positives and false negatives is greater than 25% of the total prediction. Besides, 11.5% of the study area is simulated as potentially frozen (726,397 pixels of the prediction grid with $p > 0.5$).

The prediction of the permafrost occurrence with RF was performed with the same sub-set used for LR. The variability of the OOB error was analyzed in order to select the correct number of trees to use. As Fig. 6 illustrates, the out-of-bag error becomes stable between 200 and 250 trees. We decided thus to use 300 trees for the RF modelling configuration.

Obtained classification AUROC is 0.884 and around 20% of the total number of observations correspond to false positives and false negatives. A total of 793,117 pixels were predicted with a positive occurrence of permafrost, that is 12.6% of the area of interest. The extent of the permafrost presence ($p > 0.5$) is thus slightly greater than the one obtained with Logistic regression. The number of expected false positives also decreases with this algorithm. Compared to the map of the permafrost distribution produced with LR, RF map is less smooth, with the presence of some spatial artefacts, which is a common issue encountered when using this technique (Brenning, 2005). However, it is worth mentioning that permafrost lower limits are visually located at the same altitude to the ones obtained with LR (see Fig. 5 A and B).

A RBF kernel was selected as a kernel function for the non-linear SVM classification, accordingly to results obtained in a preliminary test study of Deluigi and Lambiel (2012). After the cross-validation step, the kernel parameters, as well as the regularization parameter C and the threshold ξ, were optimized via grid search. The number of support vectors is close to the 39% of the training observations (around 36,000 samples). This value is not only dependent on how much slack is allowed, but also on the complexity of the model. To allow users interpreting the binary result provided by SVM in a meaningful way, the classification of presence and absence of permafrost was transformed by post-processing to yield a posteriori probability (from categorical to probabilistic prediction). The technique, presented by Platt (1999), applies a maximum likelihood-optimized logistic transformation on the SVM decision function in order to obtain permafrost probabilities. Classification AUROC of the RBF-SVM is equal to 0.848, with around 14.2% of the total prediction classified as false positives and false negatives. The number of pixels indicating a probability of permafrost occurrence greater than 0.5 is 1,079,745, which corresponds to 17.13% of the total region extent. This is reflected by a map with more extensive surface potentially occupied by permafrost.

Table 2
Summary statistics of the Logistic regression, Support Vector Machines and Random forests models.

Statistics	LR	SVM	RF
Precision	0.743	0.858	0.797
Recall	0.746	0.859	0.798
AUROC	0.807	0.848	0.884
FP (%)	10.72	5.97	8.78
FN (%)	14.70	8.17	11.37
# cells with $p > 0.5$	726,397	1,079,745	793,117

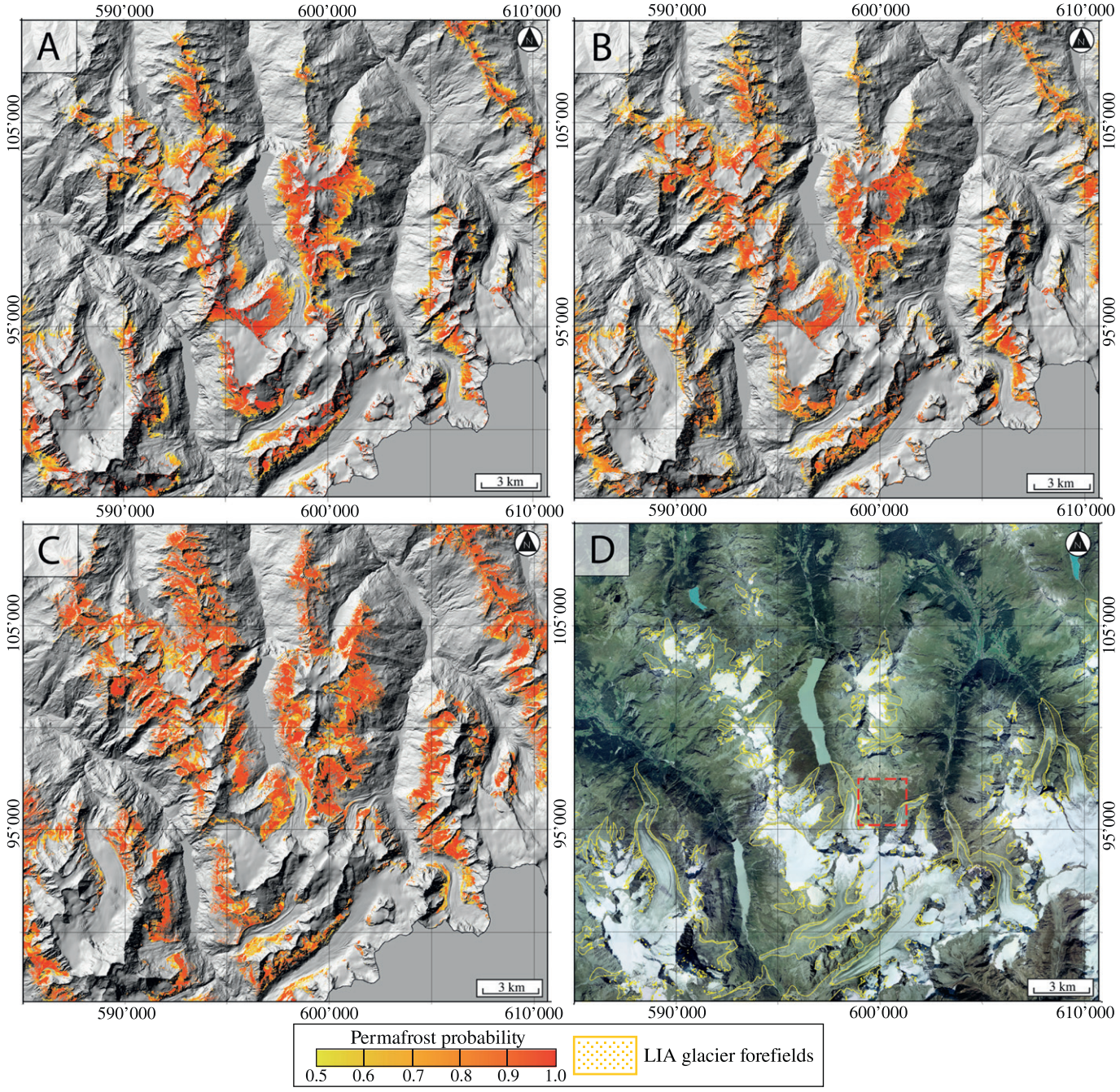

Fig. 5. Permafrost distribution maps obtained with (A) Logistic regression, (B) Random Forests and (C) Support Vector Machines. (D) Ground-truth of the study area (aerial images from swisstopo) and LIA glacier forefield extent for ease of interpretation. Red dashed square indicates the location the overviews of the Fig. 8.

3.2. Model comparison

It is common practice in machine learning to estimate the classification error by using cross-validation and to choose the algorithm that provides the lowest estimate. However, it is important to investigate which model is statistically the best when performing a specific classification task. ROC curves (Fig. 7) were evaluated on independent test sets for comparing the generalization performances of LR, SVM and RF.

Resulting performances were compared by using the Model Evaluator module of WEKA (see Witten and Frank, 2005) that employs a paired *t*-test(confidence: 0.05, two tailed) (Table 3). Results of the test indicate that SVM is not significantly worse than RF. However, the paired *t*-test outcome suggests that RF is significantly better than LR.

3.3. Expert domain quality evaluation

In addition to the statistical evaluation of the presented models, the three maps were also analyzed according to their geomorphological relevance. The lower limit of permafrost given by SVM is 100–150 m lower than the one given by LR and RF, being more in accordance with field observations (see Fig. 8 A, B and C). SVM probabilities appear to be generally higher than the ones given by LR and RF. In comparison with the permafrost map of the Swiss Federal Office for the Environment (BAFU, 2005) or the Alpine Permafrost Index Map (APIM) of Boeckli et al. (2012), the proposed simulations provide less optimistic results. Indeed, especially for LR and RF, the prediction of the presence of permafrost in sediments is restricted to smaller surfaces. In addition, maps produced by using machine

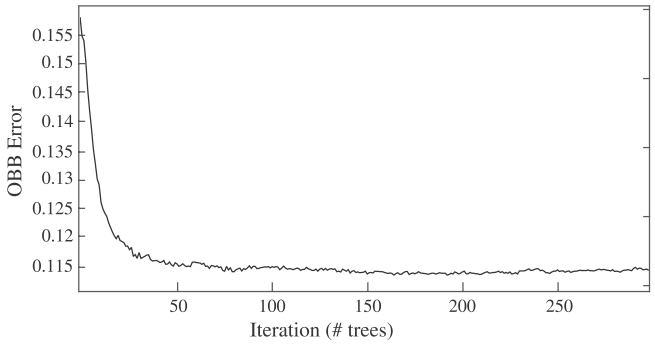

Fig. 6. OBB error as a function of the number of trees.

learning do not present the typical altitude thresholds that indicate higher permafrost occurrence with the increase in altitude (see Lambiel and Reynard, 2001; BAFU, 2005; Schrott et al., 2012; Boeckli et al., 2012). As the relationship between permafrost evidences and environmental predictors is learnt directly from data without recurring to physical models, probabilities are predicted for each independent pixel. Machine learning algorithms appear thus more suitable to simulate the high spatial discontinuity of the phenomenon at the micro-scale.

Despite the conservative result in terms of surfaces potentially frozen and a slightly lower AUROC compared to RF, SVM granted a classification with the lowest number of miss-classifications. Obtained AUROCs range mid-way between existing studies such as Boeckli et al. (2012), Azócar et al. (2016) and Sattler et al. (2016). This may be explained by the addition to the adopted dataset of indicators of know permafrost absence not only restricted to relict rock glacier, but also in talus slopes and other sediment accumulations.

When observing the interpretability of the proposed maps, the RF map is less smooth than the LR and SVM ones and presents a higher number of artefacts. Conversely, SVM gives less variability of probability when observing a given pixel and the one in the neighborhood. Furthermore, the potential distribution of permafrost is more conservative with this approach. Its great heterogeneity is also better respected with SVM. In fact, LR produces probabilities higher than 0.5 that increase linearly with the altitude. If the permafrost probability increases effectively with the altitude at the regional scale, permafrost occurrence at the local scale can change within distances of few tens of meters due to the high variability of the local characteristics (see Otto et al., 2012; Rödder and Kneisel, 2012). In some talus slopes, the SVM map illustrates a lower probability in the mid-upper part of the slope

Table 3
Model performances and paired *t*-test outcomes (v: significantly better, *: significantly worse).

Classifier	SVM	RF	LR
Performance (AUROC)	0.848 (v/ /*)	0.884 (0/1/0)	0.807* (0/0/1)

(Fig. 8 C). As showed by Lambiel and Pieracci (2008) or Scapozza et al. (2011) this distribution is more in accordance with the field reality. The same behaviour is also partially simulated with LR and RF, but their result is less conservative and it presents an increased number of false positives and false negatives. In glacier forefields, highlighted with a yellow mask in Fig. 5 D), the permafrost distribution may be even more complex due to thermal and mechanical perturbations by the glacier advance during the Little Ice Age (Reynard et al., 2003; Kneisel and Kääb, 2007). These studies illustrated that permafrost is often restricted to the lateral and frontal margin of these environments, where the former glacier was the thinnest. Hence, one has to be careful when looking at the potential permafrost extent within these areas.

4. Conclusions

In this study, we presented the results of the classification and mapping of mountain permafrost data using Logistic regression (LR), Random forests (RF) and Support Vector Machines (SVM) in a large area of the Western Swiss Alps. Machine learning algorithms provided precise distribution maps at the micro-scale by learning the statistical relationship between training permafrost evidences and permafrost explanatory variables. LR predicted a smooth map with an increase of the permafrost probability linearly with the altitude, which does not reflect the strong spatial discontinuity of the phenomenon. RF provided excellent classification performances despite the similar permafrost extent of the LR map, but it differs in terms of the result smoothness. SVM model performance resides between the two other applied classifiers. It is characterized by a lower number of miss-classifications and the potential permafrost map obtained tends to be more conservative in comparison to LR and RF. In addition, the permafrost discontinuity was best reproduced with SVM. Conversely to LR, the occurrence of permafrost does not tend to increase linearly with the altitude and it is indeed possible to observe higher permafrost probabilities in the lower half of some talus slopes, which is in agreement with field data.

The internal mechanisms of the three employed classification algorithms open the way to further analysis on permafrost data such

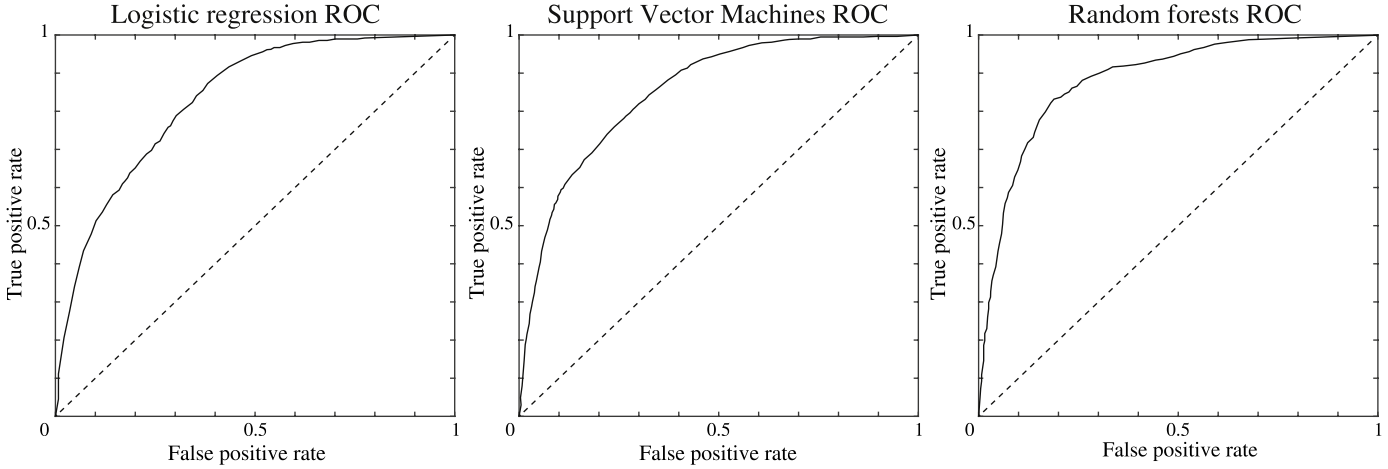

Fig. 7. ROC curves for classification by Logistic regression (0.807, left), Support Vector Machines (0.848, center) and Random forests (0.884, right).

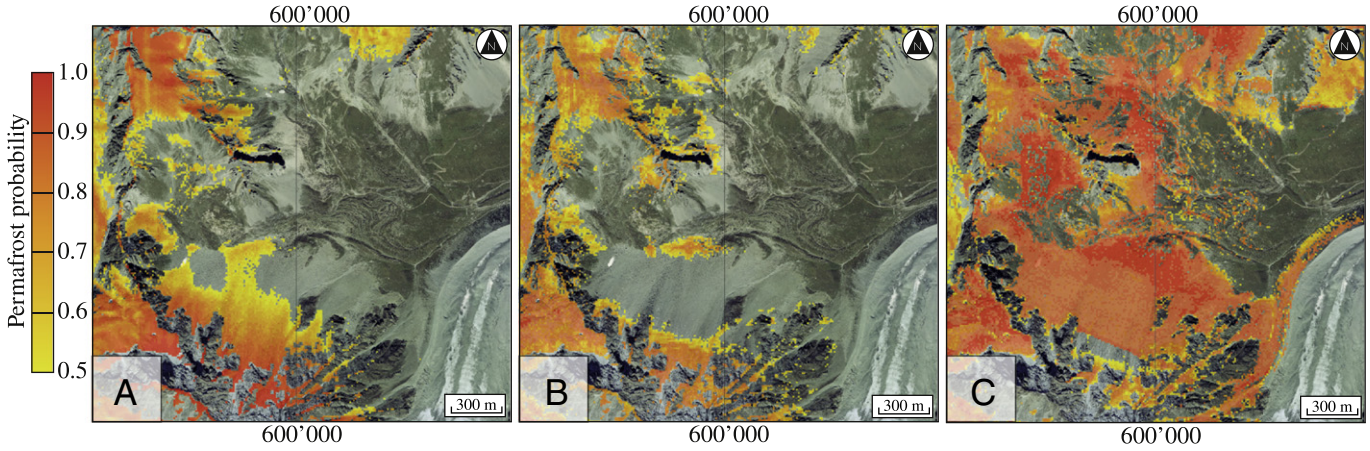

Fig. 8. Potential permafrost distribution in the Fontanesses sector (Arolla Valley) obtained with (A) Logistic regression, (B) Random forests and (C) Support Vector Machines.

as active learning, allowing choosing training data from selected support vectors, and featuring ranking, with embedded measures of the variable importance. It follows that the approach presented not only helps in mapping the mountain permafrost distribution but can also be employed to understand related data properties. Much research remains thus to be done to improve the prediction at the micro-scale. For example, model uncertainties characterization could reduce miss-classification of known permafrost evidences and thus improve the model robustness. The extraction of new environmental variables controlling permafrost conditions at the micro-scale, such as the grain size of sedimentary deposits, could as well help refining obtained results.

Acknowledgments

We thank two anonymous reviewers for their constructive comments. We would also like to acknowledge the Swiss National Science Foundation for the funding of this research (project no. 200021_152924) as well as Prof. R. Delaloye and colleagues from the University of Fribourg for having provided permafrost evidences.

References

Altman, N.S., 1992. An introduction to kernel and nearest-neighbor nonparametric regression. Am. Stat. 46 (3), 175–185.
Amatulli, G., Camia, A., San-Miguel-Ayanz, J., 2013. Estimating future burned areas under changing climate in the EU-Mediterranean countries. Sci. Total. Environ. 450, 209–222.
Avian, M., Kellerer-Pirklbauer, A., 2012. Modelling of potential permafrost distribution during the Younger Dryas, the Little Ice Age and at present in the Reisseck Mountains, Hohe Tauern Range, Austria. Aust. J. Earth Sci. 105 (2), 140–153.
Azócar, G.F., Brenning, A., Bodin, X., 2016. Permafrost distribution modeling in the semi-arid Chilean Andes. Cryosphere Discuss. 2016, 1–25.
BAFU, 2005. Hinweiskarte der potenziellen Permafrostverbreitung der Schweiz. Bundesamt für Umwelt.
Barboux, C., Delaloye, R., Lambiel, C., 2014. Inventorying slope movements in an Alpine environment using DInSAR. Earth Surf. Process. Landf. 39 (15), 2087–2099.
Barsch, D., 2012. Rockglaciers: indicators for the present and former geoecology in high mountain environments. vol. 16. Springer Science & Business Media.
Beniston, M., Farinotti, D., Stoffel, M., Andreassen, L.M., Coppola, E., Eckert, N., Fantini, A., Giacona, F., Hauck, C., Huss, M., Huwald, H., Lehning, M., López-Moreno, J.-I., Magnusson, J., Marty, C., Moran-Tejéda, E., Morin, S., Naaim, M., Provenzale, A., Rabatel, A., Six, D., Stötter, J., Strasser, U., Terzago, S., Vincent, C., 2017. The European mountain cryosphere: a review of past, current and future issues. Cryosphere Discuss. 2017, 1–60.
Bishop, C.M., 2006. Pattern recognition. Mach. Learn. 128,
Boeckli, L., Brenning, A., Gruber, S., Noetzli, J., 2012. A statistical approach to modelling permafrost distribution in the European Alps or similar mountain ranges. Cryosphere 6 (1), 125–140.
Bosson, J.-B., Deline, P., Bodin, X., Schoeneich, P., Baron, L., Gardent, M., Lambiel, C., 2015. The influence of ground ice distribution on geomorphic dynamics since the Little Ice Age in proglacial areas of two cirque glacier systems. Earth Surf. Process. Landf. 40 (5), 666–680.
Bouët, M., 1978. Le Valais. Klimatologie der Schweiz 2. Régionale Beschreibungen. 1. Teil. Beih. Ann. Schweiz. Meteorolog. Zentralanst 1977, 88–114.
Breiman, L., 2001. Random forests. Mach. Learn. 45 (1), 5–32.
Brenning, A., 2005. Spatial prediction models for landslide hazards: review, comparison and evaluation. Nat. Hazards Earth Syst. Sci. 5 (6), 853–862.
Brenning, A., Trombotto, D., 2006. Logistic regression modeling of rock glacier and glacier distribution: topographic and climatic controls in the semi-arid Andes. Geomorphology 81 (1), 141–154.
Carturan, L., Zuecco, G., Seppi, R., Zanoner, T., Borga, M., Carton, A., Dalla Fontana, G., 2015. Catchment-scale permafrost mapping using spring water characteristics. Permafr. Periglac. Process. 27 (3), 253–270.
Catani, F., Lagomarsino, D., Segoni, S., Tofani, V., 2013. Landslide susceptibility estimation by random forests technique: sensitivity and scaling issues. Nat. Hazards Earth Syst. Sci. 13 (11), 2815–2831.
Chang, C.-C., Lin, C.-J., 2011. LIBSVM: a library for support vector machines. ACM Trans. Intell. Syst. Technol. (TIST) 2 (3), 27.
Cherkassky, V., Mulier, F., 2007. Learning From Data: Concepts, Theory, and Methods. John Wiley & Sons.
Cutler, D.R., Edwards, T.C., Beard, K.H., Cutler, A., Hess, K.T., Gibson, J., Lawler, J.J., 2007. Random forests for classification in ecology. Ecology 88 (11), 2783–2792.
Davies, D.L., Bouldin, D.W., 1979. A cluster separation measure. IEEE Trans. Pattern Anal. Mach. Intell. 2, 224–227.
Delaloye, R., 2004. Contribution à l'étude du PergéLisol de Montagne en Zone Marginale. Université de Fribourg. Ph.D. thesis
Delaloye, R., Lambiel, C., 2005. Evidence of winter ascending air circulation throughout talus slopes and rock glaciers situated in the lower belt of alpine discontinuous permafrost (Swiss Alps). Nor. Geogr. Tidsskr. 59 (2), 194–203.
Delaloye, R., Lambiel, C., 2008. Typology of vertical electrical soundings for permafrost/ground ice investigation in the forefields of small alpine glaciers. In: Hauck, C., Kneisel, C. (Eds.), Applied Geophysics in Periglacial Environments. Cambridge University Press., pp. 101–108.
Delaloye, R., Lambiel, C., Gärtner-Roer, I., 2010. Overview of rock glacier kinematics research in the Swiss Alps: seasonal rhythm, interannual variations and trends over several decades. Geographica Helvetica 65 (2), 135–145.
Delaloye, R., Lambiel, C., Lugon, R., Raetzo, H., Strozzi, T., 2007. Typical ERS InSAR signature of slope movements in a periglacial mountain environment (Swiss Alps). Proceedings envisat symposium. vol. ESA SP-636. Montreux, Switzerland.
Delaloye, R., Morand, S., 1998. Les glaciers rocheux de la région d'Entremont (Alpes valaisannes): inventaire et analyse spatiale à l'aide d'un SIG. Mitteilungen der versuchsantalt für wasserbau, hydrologie und glaziologie. vol. 158. ETH Zürich., pp. 75–86.
Deluigi, N., Lambiel, C., 2012. PERMAL: a machine learning approach for alpine permafrost distribution modeling. In: Graf, C. (Ed.), Mattertal - ein tal in bewegung. Jahrestagung der schweizerischen geomorphologischen gesellschaft. vol. 4. pp. 47–62.
Doswell, C.A., I.I.I., Davies-Jones, R., Keller, D.L., 1990. On summary measures of skill in rare event forecasting based on contingency tables. Weather Forecast. 5 (4), 576–585.
Ebohon, B., Schrott, L., 2008. Modeling Mountain Permafrost Distribution: A New Permafrost Map of Austria. In: Kane, D., Hinkel, K. (Eds.), Proceedings of the Ninth International Conference on Permafrost. pp. 397–402. Fairbanks, Alaska.
Etzelmüller, B., Frauenfelder, R., 2009. Factors controlling the distribution of mountain permafrost in the Northern Hemisphere and their influence on sediment transfer. Arct. Antarct. Alp. Res. 41 (1), 48–58.
Etzelmüller, B., Hoelzle, M., Flo Heggem, E.S., Isaksen, K., Mittaz, C., Mühll, D.V., Ødegård, R.S., Haeberli, W., Sollid, J.L., 2001. Mapping and modelling the occurrence and distribution of mountain permafrost. Nor. Geogr. Tidsskr. Norwegian J. Geogr. 55 (4), 186–194.
Everitt, B.S., Landau, S., Leese, M., Stahl, D., 2011. Miscellaneous clustering methods. 5th ed., Cluster Analysis , pp. 215–255
Fawcett, T., 2006. An introduction to ROC analysis. Pattern Recogn. Lett. 27 (8), 861–874.

Friedman, J.H., 1989. Regularized discriminant analysis. J. Am. Stat. Assoc. 84 (405), 165–175.
Gruber, S., Haeberli, W., 2007. Permafrost in steep bedrock slopes and its temperature-related destabilization following climate change. J. Geophys. Res. Earth Surf. (2003-2012) 112 (F2).
Gruber, S., Hoelzle, M., Haeberli, W., 2004. Rock-wall temperatures in the Alps: modelling their topographic distribution and regional differences. Permafr. Periglac. Process. 15 (3), 299–307.
Guglielmin, M., Aldighieri, B., Testa, B., 2003. PERMACLIM: a model for the distribution of mountain permafrost, based on climatic observations. Geomorphology 51 (4), 245–257.
Haeberli, W., 1975. Untersuchungen zur Verbreitung von Permafrost zwischen Flüelapass und Piz Grialetsch (Graubünden). Versuchsanstalt für Wasserbau, Hydrologie und Glaziologie.
Haeberli, W., 1985. Creep of mountain permafrost: internal structure and flow of alpine rock glaciers. Mitteilungen der Versuchsanstalt fur Wasserbau, Hydrologie und Glaziologie an der ETH Zurich 77, 5–142.
Hall, M., Frank, E., Holmes, G., Pfahringer, B., Reutemann, P., Witten, I.H., 2009. The WEKA data mining software: an update. ACM SIGKDD Explorations Newsl. 11 (1), 10–18.
Harris, C., Arenson, L., Christiansen, H.H., Etzelmuller, B., Frauenfelder, R., Gruber, S., Haeberli, W., Hauck, C., Hoelzle, M., Humlum, O., Isaksen, K., Kääb, A., Kern-Luetschg, M., Lehning, M., Matsuoka, N., Murton, J.B., Noezli, J., Phillips, M., Ross, N., Seppala, M., Springman, S.M., Vonder Muehll, D., 2009. Permafrost and climate in Europe: monitoring and modelling thermal, geomorphological and geotechnical responses. Earth Sci. Rev. 92 (3), 117–171.
Harris, C., Murton, J., 2005. Interactions between glaciers and permafrost: an introduction. Geol. Soc. Spec. Pub. 242, 1–9.
Hastie, T., Tibshirani, R., Friedman, J., 2009. Unsupervised learning. . The Elements of Statistical LearningSpringer., pp. 485–585.
Hauck, C., Kneisel, C., 2008. Electrical methods. Appl. Geophys Periglacial Environ. 3–27.
Hauck, C., Vonder Mühll, D., Maurer, H., 2003. Using DC resistivity tomography to detect and characterize mountain permafrost. Geophys. Prospect. 51 (4), 273–284.
Haykin, S., 2009. Neural networks and learning machines. vol. 3. Pearson Education Upper Saddle River.
Hilbich, C., Marescot, L., Hauck, C., Loke, M., Mäusbacher, R., 2009. Applicability of electrical resistivity tomography monitoring to coarse blocky and ice-rich permafrost landforms. Permafr. Periglac. Process. 20 (3), 269–284.
Hoelzle, M., 1994. Permafrost und Gletscher im Oberengadin: Grundlagen und Anwendungsbeispiele für automatisierte Schätzverfahren. Mitteilungen der Versuchsanstalt für Wasserbau, Hydrologie und Glaziologie an der Eidgenössischen Technischen Hochschule ZürichVAW.
Hoelzle, M., Wegmann, M., Krummenacher, B., 1999. Miniature temperature dataloggers for mapping and monitoring of permafrost in high mountain areas: first experience from the Swiss Alps. Permafr. Periglac. Process. 10 (2), 113–124.
Hosmer, D.W., Lemeshow, S., 2000. Introduction to the logistic regression model. 2nd ed., Applied Logistic Regression , pp. 1–30
Humlum, O., 1996. Origin of rock glaciers: observations from Mellemfjord, Disko Island, central West Greenland. Permafr. Periglac. Process. 7 (4), 361–380.
Izenman, A., 2008. Modern multivariate statistical techniques: regression. Classification, and Manifold Learning Springer Texts in Statistics, New York.
Kääb, A., Frauenfelder, R., Roer, I., 2007. On the response of rock glacier creep to surface temperature increase. Global Planet. Change 56 (1), 172–187.
Kanevski, M., Pozdnoukhov, A., Timonin, V., 2009. Machine learning for spatial environmental data: theory, applications, and software. EPFL press.
Kleinbaum, D., Klein, M., 1994. Logistic Regression: A Self-learning Text. Springer-Verlag. New York
Kneisel, C., Kääb, A., 2007. Mountain permafrost dynamics within a recently exposed glacier forefield inferred by a combined geomorphological, geophysical and photogrammetrical approach. Earth Surf. Process. Landf. 32 (12), 1797–1810.
Kobierska, F., Jonas, T., Magnusson, J., Zappa, M., Bavay, M., Bosshard, T., Paul, F., Bernasconi, S., 2011. Climate change effects on snow melt and discharge of a partly glacierized watershed in Central Switzerland (SoilTrec Critical Zone Observatory). Appl. Geochem. 26, S60–S62.
Kohonen, T., 1982. Self-organized formation of topologically correct feature maps. Biol. Cybern. 43 (1), 59–69.
Kohonen, T., Honkela, T., 2007. Kohonen network. Scholarpedia 2 (1), 1568.
Lambiel, C., 2006. Le pergélisol dans les terrains sédimentaires à forte déclivité: distribution, régime thermique et instabilités. UNIL-Faculté des géosciences et de l'environnement-Institut de géographie.
Lambiel, C., Pieracci, K., 2008. Permafrost distribution in talus slopes located within the alpine periglacial belt, Swiss Alps. Permafr. Periglac. Process. 19 (3), 293–304.
Lambiel, C., Reynard, E., 2001. Regional modelling of present, past and future potential distribution of discontinuous permafrost based on a rock glacier inventory in the Bagnes-Hérémence area (Western Swiss Alps). Nor. Geogr. Tidsskr. Norwegian J. Geogr. 55 (4), 219–223.
Lambiel, C., Reynard, E., 2003. Cartographie de la distribution du pergélisol et datation des glaciers rocheux dans la région du Mont Gelé (Valais). Phys. Geogr. 41, 91–104.
Lane, S., Tayefi, V., Reid, S., Yu, D., Hardy, R., 2007. Interactions between sediment delivery, channel change, climate change and flood risk in a temperate upland environment. Earth Surf. Process. Landf. 32 (3), 429–446.
Le Cessie, S., Van Houwelingen, J., 1994. Logistic regression for correlated binary data. Appl. Stat. 43, 95–108.
Luoto, M., Hjort, J., 2005. Evaluation of current statistical approaches for predictive geomorphological mapping. Geomorphology 67 (3), 299–315.
Magnin, F., Brenning, A., Bodin, X., Deline, P., Ravanel, L., 2015. Statistical modelling of rock wall permafrost distribution: application to the Mont Blanc massif. Geomorphologie Paris, 20.
Marescot, L., Loke, M., Chapellier, D., Delaloye, R., Lambiel, C., Reynard, E., 2003. Assessing reliability of 2D resistivity imaging in mountain permafrost studies using the depth of investigation index method. Near Surf. Geophys. 1 (2), 57–67.
Marmion, M., Hjort, J., Thuiller, W., Luoto, M., 2008. A comparison of predictive methods in modelling the distribution of periglacial landforms in Finnish Lapland. Earth Surf. Process. Landf. 33 (14), 2241–2254.
McLachlan, G., 2004. Discriminant analysis and statistical pattern recognition. vol. 544. John Wiley & Sons.
Micheletti, N., Foresti, L., Robert, S., Leuenberger, M., Pedrazzini, A., Jaboyedoff, M., Kanevski, M., 2014. Machine learning feature selection methods for landslide susceptibility mapping. Math. Geosci. 46 (1), 33–57.
Mittaz, C., Imhof, M., Hoelzle, M., Haeberli, W., 2002. Snowmelt evolution mapping using an energy balance approach over an Alpine terrain. Arct. Antarct. Alp. Res. 34 (3), 274–281.
Morand, S., 2000. Inventaire des glaciers rocheux du Val d'Arolla. Rapport interne, Service des forê,ts et du paysage du Canton du Valais, Sion.
Noetzli, J., Gruber, S., Kohl, T., Salzmann, N., Haeberli, W., 2007. Three-dimensional distribution and evolution of permafrost temperatures in idealized high-mountain topography. J. Geophys. Res. Earth Surf. (2003-2012) 112 (F2).
Otto, J., Keuschnig, M., Goetz, J., Marbach, M., Schrott, L., 2012. Detection of mountain permafrost by combining high resolution surface and subsurface information—an example from the Glatzbach catchment, Austrian Alps. Geogr. Ann. Ser. A Phys. Geogr. 94 (1), 43–57.
Otto, J., Sass, O., 2006. Comparing geophysical methods for talus slope investigations in the Turtmann Valley (Swiss Alps). Geomorphology 76 (3), 257–272.
Ou, C., LaRocque, A., Leblon, B., Zhang, Y., Webster, K., McLaughlin, J., 2016. Modelling and mapping permafrost at high spatial resolution using Landsat and Radarsat-2 images in Northern Ontario, Canada: part 2—regional mapping. Int. J. Remote Sens.
PERMOS, Noetzli, J., Luethi, R., Staub, B. (Eds.), 2016. Permafrost in Switzerland 2010/2011 to 2013/2014. Glaciological Report (Permafrost) No. 12-15 of the Cryospheric Commission of the Swiss Academy of Sciences.
Platt, J., 1999. Probabilistic outputs for support vector machines and comparisons to regularized likelihood methods. Adv. Large Margin Classifiers 10 (3), 61–74.
Ravanel, L., Allignol, F., Deline, P., Gruber, S., Ravello, M., 2010. Rock falls in the Mont Blanc Massif in 2007 and 2008. Landslides 7 (4), 493–501.
Reynard, E., Lambiel, C., Delaloye, R., Devaud, G., Baron, L., Chapellier, D., Marescot, L., Monnet, R., 2003. Glacier/permafrost relationships in forefields of small glaciers (Swiss Alps). Proceedings 8th international conference on permafrost, Zurich, Switzerland. vol. 2. pp. 947–952.
Ribolini, A., Guglielmin, M., Fabre, D., Bodin, X., Marchisio, M., Sartini, S., Spagnolo, M., Schoeneich, P., 2010. The internal structure of rock glaciers and recently deglaciated slopes as revealed by geoelectrical tomography: insights on permafrost and recent glacial evolution in the Central and Western Alps (Italy–France). Quat. Sci. Rev. 29 (3), 507–521.
Rödder, T., Kneisel, C., 2012. Influence of snow cover and grain size on the ground thermal regime in the discontinuous permafrost zone, Swiss Alps. Geomorphology 175, 176–189.
Roer, I., Haeberli, W., Avian, M., Kaufmann, V., Delaloye, R., Lambiel, C., Kääb, A., 2008. Observations and considerations on destabilizing active rock glaciers in the European Alps. Ninth international conference on permafrost. vol. 2. pp. 1505–1510.
Sattler, K., Anderson, B., Mackintosh, A., Norton, K., de Róiste, M., 2016. Estimating permafrost distribution in the maritime southern Alps, New Zealand, based on climatic conditions at rock glacier sites. Front. Earth Sci. 4, 4.
Scapozza, C., 2013. Stratigraphie, Morphodynamique, Paléoenvironnements des Terrains Sédimentaires Meubles À Forte déclivité du Domaine Périglaciaire Alpin. Université de Lausanne. Ph.D. thesis.
Scapozza, C., Lambiel, C., Baron, L., Marescot, L., Reynard, E., 2011. Internal structure and permafrost distribution in two alpine periglacial talus slopes, Valais, Swiss Alps. Geomorphology 132 (3), 208–221.
Schöner, W., Boeckli, L., Hausmann, H., Otto, J.-C., Reisenhofer, S., Riedl, C., Seren, S., 2012. Spatial patterns of permafrost at Hoher Sonnblick (Austrian Alps)—extensive field-measurements and modelling approaches. Aust. J. Earth Sci. 105 (2), 154–168.
Schrott, L., Otto, J.-C., Keller, F., 2012. Modelling alpine permafrost distribution in the Hohe Tauern region, Austria. Aust. J. Earth Sci. 105 (2), 169–183.
Staub, B., Marmy, A., Hauck, C., Hilbich, C., Delaloye, R., 2015. Ground temperature variations in a talus slope influenced by permafrost: a comparison of field observations and model simulations. Geogr. Helv. 70 (1), 45–62.
Swets, J.A., 1988. Measuring the accuracy of diagnostic systems. Science 240 (4857), 1285–1293.
Trigila, A., Iadanza, C., Esposito, C., Scarascia-Mugnozza, G., 2015. Comparison of logistic regression and Random forests techniques for shallow landslide susceptibility assessment in Giampilieri (NE Sicily, Italy). Geomorphology 249, 119–136.
Vapnik, V., 1998. Statistical Learning Theory. Wiley, New York.
Varley, A., Tyler, A., Smith, L., Dale, P., Davies, M., 2016. Mapping the spatial distribution and activity of 226Ra at legacy sites through Machine Learning interpretation of gamma-ray spectrometry data. Sci. Total. Environ. 545, 654–661.
Witten, I.H., Frank, E., 2005. Data Mining: Practical Machine Learning Tools and Techniques. Morgan Kaufmann.